Available online at www.sciencedirect.com
SCIENCE DIRECT®
Computers and Electronics in Agriculture 46 (2005) 135–152
Computers and electronics in agriculture
www.elsevier.com/locate/compag

Characterizing soil spatial variability with apparent soil electrical conductivity Part II. Case study

D.L. Corwin*, S.M. Lesch

USDA-ARS, George E. Brown Jr. Salinity Laboratory, 450 West Big Springs Road, Riverside, CA 92507-4617, USA

Abstract

Geospatial measurements of apparent soil electrical conductivity (EC_a) are recognized as a means of characterizing soil spatial variability at field and landscape scales. However, inconsistencies in the measurement and interpretation of field- and landscape-scale geospatial EC_a measurements have resulted in data sets that are unreliable and/or incompatible. These inconsistencies are, in part, a consequence of the lack of EC_a-survey protocols that provide standardized guidelines to assure reliability, consistency, and compatibility. It is the objective of this paper to apply EC_a-survey protocols to a soil quality assessment to demonstrate their utility in characterizing spatial variability. The soil quality assessment was conducted on a 32.4-ha field on the westside of central California's San Joaquin Valley where a mobile electromagnetic induction (EM) survey was performed following outlined protocols. The EM survey consisted of EC_a measurements taken at 22,177 locations in April 2002. A response-surface sampling design was used to identify 40 sites where soil-core samples were taken at 0.3-m increments to a depth of 1.2 m. Duplicate samples were taken at eight sites to evaluate the local-scale variability. Soil samples were analyzed for a variety of physico-chemical properties associated with soil quality for an arid zone soil. Analysis characterized the soil as montmorillonitic, saline, and sodic

Abbreviations: ANOVA, analysis of variance; CEC, cation exchange capacity; CV, coefficient of variation; EC_a, apparent soil electrical conductivity; EC_e, electrical conductivity of the saturation extract; EM, electromagnetic induction; EM_h, electromagnetic induction measurement in the horizontal coil-mode configuration; EM_v, electromagnetic induction measurement in the vertical coil-mode configuration; ESAP, EC_e sampling, assessment and prediction software; ESP, exchangeable sodium percentage; GIS, geographic information system; GPS, global positioning system; IDW, inverse distance weighting; K_s, saturated hydraulic conductivity; SAR, sodium adsorption ratio; SP, saturation percentage; WSJV, western San Joaquin Valley

* Corresponding author. Tel.: +1 951 369 4819; fax: +1 951 342 4962.
E-mail address: dcorwin@ussl.ars.usda.gov (D.L. Corwin).

0168-1699/$ – see front matter. Published by Elsevier B.V.
doi:10.1016/j.compag.2004.11.003

with EC_e (electrical conductivity of the saturation extract) varying from 4.83 to 45.3 dS m^{-1}, SAR (sodium adsorption ratio) from 5.62 to 103.12, and clay content from 2.5 to 48.3%. Spatial trends showed high areas of salinity and SAR in the center of the southern half of the study area. Strong correlation was obtained between EC_a and the soil properties of the saturation extract (EC_e; Cl^-, HCO_3^-, SO_4^{2-}, Na^+, K^+, and Mg^{2+}), exchangeable Na^+, and SAR. Other properties were poorly correlated, including: volumetric water content (θ_v), bulk density (D_b), percent clay (% clay), saturation percentage (SP), exchangeable sodium percentage (ESP), Mo, $CaCO_3$, gypsum, total N, Ca^{2+} in the saturation extract, and exchangeable cations (K^+, Ca^{2+}, and Mg^{2+}). The spatial distribution of the poorly correlated properties is not as well represented with a response-surface sampling design suggesting the need for a complementary stratified random sample design.
Published by Elsevier B.V.

Keywords: EC_a; Electromagnetic induction; Salinity; San Joaquin Valley; Spatial heterogeneity; Soil quality

1. Introduction

The use of apparent soil electrical conductivity (EC_a) in agriculture has evolved from a tool for measuring soil salinity to a means of mapping spatial variability of soil physico-chemical properties for applications in solute transport modeling, soil quality assessment, and precision agriculture (Corwin and Lesch, 2005a). However, the use of geospatial measurements of EC_a in agriculture has suffered from problems stemming, in part, from a lack of standardized procedures. Concerns over consistency, reliability, and compatibility led to papers by Sudduth et al. (2001) and Corwin and Lesch (2003) regarding accuracy issues and guidelines, respectively. These papers were the precursors to the development of EC_a-survey protocols by Corwin and Lesch (2005b). To demonstrate the utility of these protocols in characterizing spatial variability, a soil quality assessment was conducted in the San Joaquin Valley.

The Sacramento and San Joaquin Valleys comprise the Central Valley of California, which is one of the most agriculturally productive areas in the world. Due to the lack of an outlet for drainage water in the western San Joaquin Valley (WSJV), continued agricultural productivity is threatened on hundreds of thousands of hectares. It is estimated that the soil quality of 300,000 ha in the WSJV may be adversely affected by the presence of shallow or perched water (0.3–1.5 m) and continued deterioration is expected. Reliable, timely, and cost-effective soil quality assessments are needed to establish inventories of salt-affected soils in the WSJV and to evaluate temporal changes. An understanding of the extent of the problem and rate of deterioration is basic information needed to evaluate the severity of the problem and to make ameliorative recommendations.

A case study of a soil quality assessment for the WSJV using EC_a-survey data to direct soil sampling is presented to provide comparative soil quality information for the WSJV and to demonstrate the effectiveness of EC_a-survey protocols in characterizing soil spatial variability. It is the objective of this paper to present a case study that illustrates the use of EC_a-survey protocols to characterize spatial variability for a soil quality assessment of saline-sodic soil.

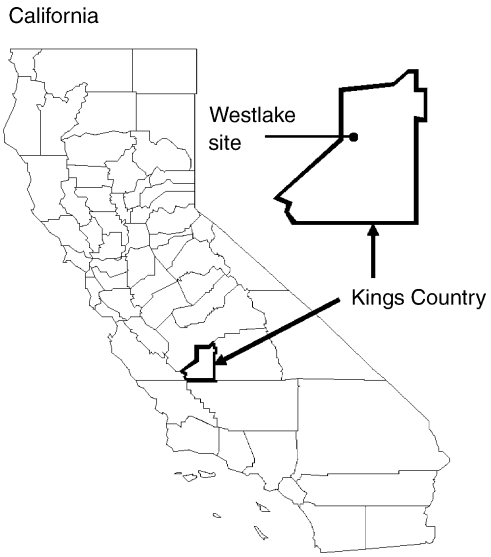

Fig. 1. Map showing the geographic location of the Westlake Farm case study site.

2. Materials and methods

2.1. Study site description

The study site is located on Westlake Farms, which resides in Kings County on the westside of California's San Joaquin Valley (Fig. 1). The soil at the Westlake Farm site is part of the Lethent clay loam series (USDA, 1986), a fine, montmorillonitic, thermic, Typic Natrargid according to Soil Survey Staff (1999). The site is a 32.4-ha field that has been prepared as a drainage water reuse study area where forage is grown to feed livestock. Within the field, eight 4-ha rectangular paddocks (or plots) with dimensions of 75 m × 364 m were laid out with their borders defined by earth berms (Fig. 2). Paddock 1 is in the southern-most part of the field, with paddock 8 in the north. Further details of the site can be found in Kaffka et al. (2002).

2.2. Soil quality assessment

The soil quality assessment consisted of four parts: (i) an intensive EC_a survey, (ii) a response-surface sampling design, (iii) soil physico-chemical analyses of soil quality properties for an arid-zone soil, and (iv) geographic information system (GIS) database development to visually display maps.

2.2.1. Intensive EM survey

The EC_a survey followed the detailed survey protocols pertaining to soil quality assessment as described within Part I. The EC_a survey was conducted from 8 to 12 April 2002.

The survey consisted of EC_a measurements taken with mobile EM equipment using the Geonics dual-dipole EM-38 soil electrical conductivity meter. Measurements were taken roughly 4 m apart. A total of 22,177 EC_a measurements were taken across the 32.4-ha study area. All measurements were geo-referenced with a global positioning system (GPS) receiver.

2.2.2. Soil sampling design

Utilizing the data from the EM survey and response-surface sampling design software (ESAPv2.0) developed by Lesch et al. (1995a,b, 2000), 40-soil sample sites were selected that characterized the spatial variability in EC_a both across each paddock and over the entire field. The sample design was generated from EC_a data collected for the entire field rather than separating the data by paddock. This provided a more reasonable statistical representation of the field-scale spatial variability, but resulted in a non-uniform number of sample sites per paddock.

Conceptually, 40 sites were chosen to satisfy the following three criteria: (i) to represent about 95% of the observed range in the geometric mean EM data, (ii) to represent about 95% of the observed range in the EM profile ratio data, and (iii) to be spatially distributed across the eight paddocks in an approximately uniform manner with 4–6 sites within each paddock (see Fig. 2). More specific details on how a spatial response-surface sampling design can be used to simultaneously achieve these criteria can be found in Lesch et al. (1995b, 2000).

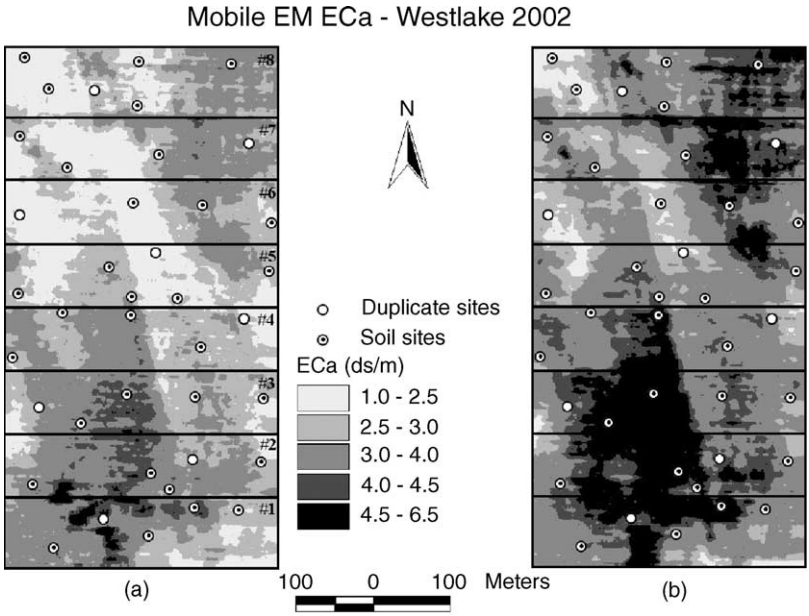

Fig. 2. Site layout map showing 2002 EM EC_a-survey measurements including (a) EM_h and (b) EM_v, paddock boundaries with paddock numbers, selected soil-core sites (bull's eye circle, ◎), and duplicate soil-core sites (empty circle, ○).

Soil cores were taken the week following the EC_a survey (i.e., 15–17 April 2002). No irrigation or precipitation occurred during the time between the EC_a survey and the soil sampling. Soil cores were taken at 0.3-m increments to a depth of 1.2 m. Within each paddock, one site was selected where duplicate soil-core samples were taken to establish local-scale variability. Duplicate soil cores were taken at eight sites (Fig. 2). A total of 192 soil samples were taken (160 soil property samples and 32 duplicate soil property samples). Fig. 2 shows the 40 selected soil-core sites and the eight duplicate soil-core sites.

2.2.3. Soil chemical and physical analyses

Various chemical properties related to soil quality for an arid-zone soil were determined for the 192 soil samples: total C and N, electrical conductivity of the saturation extract (EC_e); pH_e; anions (HCO_3^-, Cl^-, NO_3^-, and SO_4^{2-}) and cations (Na^+, K^+, Ca^{2+}, and Mg^{2+}) in the saturation extract; trace elements (B, Se, As, and Mo) in the saturation extract; $CaCO_3$; gypsum; cation exchange capacity (CEC); exchangeable Na^+, K^+, Mg^{2+}, and Ca^{2+}; exchangeable sodium percentage (ESP); and sodium adsorption ratio (SAR). The 192 soil samples were also analyzed for soil physical properties including SP, volumetric water content (θ_v), bulk density (ρ_b), and clay content. The chemical and physical methods used for each analysis were from Methods of Soil Analysis Parts 1 and 2 (Page et al., 1982; Klute, 1986), except for total C and N, which were analyzed with a Leco C-N 2000 Analyzer.

Tables 1–4 are a summary of all physico-chemical analyses for the 0–0.3, 0.3–0.6, 0.6–0.9, and 0.9–1.2 m depth increments, respectively. Of all the physico-chemical properties analyzed using the analytical procedures outlined in Methods of Soil Analysis, the most difficult property to accurately determine was CEC due to the interference caused by gypsum and lime. The recommended method for calcareous and gypsiferous soils yielded the most realistic results, but still tended to underestimate CEC on about 10% of the samples. Subsequently, this produced spurious ESP calculations greater than 100%. Nevertheless, the CEC and ESP results were not eliminated from the database because it was felt that on a relative basis the information was still useful.

2.2.4. GIS and map preparation

All spatial data were entered into a GIS using the commercial software ArcView 3.3 (ESRI, 2002). Maps of the soil physico-chemical properties were prepared by interpolating the measurements at the 40-sample sites using inverse distance weighting (IDW). At this particular study site, IDW was selected as the preferred method of interpolation because it was consistently more accurate than kriging based on the use of the mean squared error as the main criterion when comparing measured to predicted values for the majority of physico-chemical properties (data not shown). Maps of EC_a measurements were also prepared.

3. Results and discussion

Fig. 2 shows an IDW interpolation at 1-m spacing of all 22,177 EM EC_a measurements taken within the study site for both EM_h and EM_v. Statistical correlations performed between EM_v EC_a and EC_e and between EM_h EC_a and EC_e for various depth increments (i.e., 0–0.3, 0.3–0.6, 0.6–0.9, 0.9–1.2, and 0–1.2 m) showed that the highest sample cor-

Table 1
Mean and range statistics for 0–0.3 m sample depth

Soil property	Mean	Minimum	Maximum	Range	S.D.	S.E.	CV	Skewness
θ_v (m^3/m^3)	0.19	0.13	0.28	0.15	0.04	0.01	18.64	0.45
ρ_b ($Mg\,m^{-3}$)	1.29	1.11	1.52	0.41	0.10	0.02	7.70	0.29
Clay (%)	35.9	22.8	48.3	25.5	6.8	1.1	19.1	−0.22
EC_e ($dS\,m^{-1}$)	11.43	4.83	30.60	25.77	6.06	0.88	53.05	1.74
pH_e	7.67	6.53	8.18	1.65	0.36	0.05	4.66	−1.80
SP (%)	64.63	48.38	80.15	31.77	9.23	1.33	14.28	0.04
SAR	23.46	5.62	59.50	53.88	14.40	2.08	61.39	1.22
ESP (%)	35.40	11.23	119.46	108.23	21.25	3.07	60.03	1.66
B ($mg\,L^{-1}$)	14.21	2.64	33.23	30.59	7.35	1.06	51.75	1.00
Mo ($\mu g\,L^{-1}$)	632.13	150.00	3291.00	3141.00	592.06	86.36	93.66	2.70
CEC (mmol/kg)	20.44	9.86	36.98	27.12	5.41	0.78	26.47	0.59
$CaCO_3$ (g/kg)[a]	1.50	0.04	5.57	5.53	1.11	0.17	74.07	1.57
Gypsum (g/kg)	3.73	0.26	10.04	9.78	2.13	0.31	57.03	0.94
Total C (g/kg)	0.81	0.30	1.13	0.83	0.20	0.03	25.13	−0.33
Total N (g/kg)	0.07	0.04	0.11	0.07	0.02	0.00	20.96	−0.03
Anions in saturation extract ($mmol\,L^{-1}$)								
HCO_3^-	2.81	1.51	5.97	4.46	0.93	0.13	32.92	1.14
Cl^-	18.30	3.14	63.68	60.54	14.38	2.08	78.60	1.75
NO_3^-	nd	nd	nd	nd	–	–	–	–
SO_4^{2-}	131.67	58.91	383.70	324.79	75.76	10.94	57.54	2.05
Cations in saturation extract ($mmol\,L^{-1}$)								
Na^+	109.54	25.05	368.29	343.25	81.38	11.75	74.29	1.80
K^+	1.41	0.56	3.11	2.55	0.52	0.08	36.85	1.21
Ca^{2+}	25.07	21.88	30.50	8.62	2.31	0.33	9.20	0.62
Mg^{2+}	15.93	9.10	54.30	45.19	9.24	1.33	58.01	3.26
Exchangeable cations (mmol/kg)								
Na^+	7.06	1.93	19.11	17.19	4.15	0.60	58.74	1.01
K^+	1.20	0.69	1.72	1.03	0.27	0.04	22.15	−0.14
Ca^{2+}	59.27	36.22	88.67	52.45	16.64	2.40	28.07	0.29
Mg^{2+}	7.10	3.97	10.12	6.15	1.41	0.20	19.92	−0.37

$N = 48$, nd: all samples below detection limits. Detection limit for NO_3 was $0.04\,mmol\,L^{-1}$.
[a] $N = 41$.

relation occurred for the composite depth increment 0–1.2 m. The correlation coefficients between EM_v EC_a and EC_e and between EM_h EC_a and EC_e for the composite 0–1.2 m depth increment are $r = 0.84$ and $r = 0.89$, respectively. This indicates that the map of EM_v EC_a in Fig. 2b most closely reflects the spatial distribution of root zone salinity. More specifically, the survey provides a detailed map of the spatial extent and magnitude of salinity in the top 1.2 m and explicitly shows the degree of spatial variability of salinity.

Apparent soil electrical conductivity data obtained with EM, as opposed to ER, are particularly useful for sample design because (i) the geometric mean (i.e., sqrt [EM_h $EC_a \times EM_v$ EC_a]) provides a measure of the cumulative EC_a through the root zone and (ii) the profile ratio mean (i.e., EM_h EC_a/EM_v EC_a) provides a means of characterizing the shape of the EC_a profile and thereby a potential means of characterizing the degree of leaching. Because both EM_v and EM_h EC_a measurements are highly correlated with EC_e, the profile ratio reveals general leaching patterns of soluble salts (Fig. 3). Areas with a profile ratio >1 indicate that the past net flow of water and salts in these ar-

Table 2
Mean and range statistics for 0.3–0.6 m sample depth

Soil property	Mean	Minimum	Maximum	Range	S.D.	S.E.	CV	Skewness
θ_v (m^3/m^3)	0.24	0.17	0.30	0.13	0.03	0.01	13.03	−0.25
ρ_b ($Mg\,m^{-3}$)	1.51	1.31	1.72	0.41	0.10	0.02	6.50	−0.03
Clay (%)	30.4	21.8	46.9	25.1	4.9	0.8	16.0	0.82
EC_e ($dS\,m^{-1}$)	17.46	6.11	34.00	27.89	6.55	0.94	37.48	0.72
pH_e	7.87	6.63	8.23	1.60	0.33	0.05	4.22	−1.96
SP (%)	67.16	50.26	86.90	36.64	10.00	1.44	14.89	0.24
SAR	40.31	9.13	78.87	69.74	15.31	2.21	37.99	0.08
ESP (%)	80.81	11.26	567.90	556.64	84.04	12.13	103.99	4.57
B ($mg\,L^{-1}$)	19.06	6.69	32.35	25.67	6.09	0.88	31.97	0.77
Mo ($\mu g\,L^{-1}$)	576.52	220.00	1783.00	1563.00	375.79	54.24	65.18	1.94
CEC (mmol/kg)	17.14	2.16	26.51	24.35	5.60	0.81	32.69	−0.25
$CaCO_3$ (g/kg)[a]	1.57	0.04	5.88	5.84	1.33	0.21	84.88	1.58
Gypsum (g/kg)	5.17	0.63	11.75	11.12	3.04	0.44	58.88	0.59
Total C (g/kg)	0.49	0.19	0.98	0.79	0.19	0.03	38.70	0.45
Total N (g/kg)	0.04	0.03	0.08	0.05	0.01	0.00	22.47	0.70
Anions in saturation extract ($mmol\,L^{-1}$)								
HCO_3^-	2.07	1.27	3.50	2.24	0.47	0.07	22.74	0.82
Cl^-	30.22	3.71	80.89	77.18	16.51	2.38	54.65	0.72
NO_3^-	nd	nd	nd	nd	–	–	–	–
SO_4^{2-}	205.18	75.99	439.80	363.81	85.77	12.38	41.80	1.21
Cations in saturation extract ($mmol\,L^{-1}$)								
Na^+	190.91	40.73	428.23	387.50	90.19	13.02	47.24	0.86
K^+	1.29	0.42	2.75	2.33	0.49	0.07	38.10	0.69
Ca^{2+}	23.73	17.88	29.64	11.76	2.22	0.32	9.36	0.59
Mg^{2+}	20.06	10.10	69.28	59.18	12.12	1.75	60.42	2.67
Exchangeable cations (mmol/kg)								
Na^+	11.04	1.85	21.00	19.15	4.16	0.60	37.69	−0.21
K^+	0.67	0.20	1.27	1.07	0.24	0.03	36.09	0.11
Ca^{2+}	72.80	33.03	130.67	97.64	26.41	3.81	36.27	0.41
Mg^{2+}	6.07	3.58	8.58	5.00	1.47	0.21	24.30	−0.03

$N = 48$, nd: all samples below detection limits. Detection limit for NO_3 was $0.04\,mmol\,L^{-1}$.
[a] $N = 41$.

eas has been upward, whereas profile ratios <1 have net downward flows. Fig. 3 shows that nearly all locations within the field have a net positive downward flow of water. Profile ratios >1 only exist in small isolated pockets in the southwestern corner of the field.

The mobile EM survey indicates a large area of very high EC_a measurements in the southwestern portion of the study area that extends through a substantial portion of paddocks 2–4 (Fig. 2). In addition, a smaller area of high EC_a exists in the northeast primarily spreading through paddocks 6–8. Figs. 3 and 4a indicate that in most locations soil salinity increases with depth. The ground-truth chemical analysis data show that the salinity profile is inverted in one small area near the southwest corner as indicated by the high EC_e measurements at 0–0.3 m overlying lower EC_e measurements at 0.3–0.6, 0.6–0.9, and 0.9–1.2 m (Fig. 4a). Specifically, inverted salinity profiles occurred at only three soil sample locations in the

Table 3
Mean and range statistics for 0.6–0.9 m sample depth

Soil property	Mean	Minimum	Maximum	Range	S.D.	S.E.	CV	Skewness
θ_v (m^3/m^3)	0.26	0.20	0.48	0.28	0.05	0.01	19.31	2.06
ρ_b ($Mg\,m^{-3}$)	1.52	1.16	1.80	0.64	0.12	0.02	8.00	−0.42
Clay (%)	26.2	2.5	42.0	39.5	6.8	1.1	25.9	−0.55
EC_e ($dS\,m^{-1}$)	22.49	7.94	37.90	29.96	6.96	1.00	30.96	0.04
pH_e	8.04	7.48	8.34	0.86	0.22	0.03	2.68	−0.89
SP (%)	64.82	48.11	117.52	69.41	14.76	2.13	22.78	1.61
SAR	53.35	16.26	91.90	75.63	16.00	2.31	30.00	−0.11
ESP (%)	81.74	13.33	179.19	165.86	36.57	5.28	44.74	0.58
B ($mg\,L^{-1}$)	21.49	11.17	34.19	23.02	5.84	0.84	27.17	0.51
Mo ($\mu g\,L^{-1}$)	661.63	252.00	2372.00	2120.00	451.51	65.17	68.24	2.15
CEC (mmol/kg)	15.05	7.74	28.53	20.79	5.04	0.73	33.52	0.79
$CaCO_3$ (g/kg)[a]	1.28	0.02	6.83	6.81	1.43	0.23	112.03	2.46
Gypsum (g/kg)	6.98	1.10	23.59	22.49	4.47	0.64	63.99	1.43
Total C (g/kg)	0.37	0.17	0.81	0.64	0.15	0.02	39.76	1.08
Total N (g/kg)	0.04	0.02	0.08	0.06	0.01	0.00	30.57	2.46
Anions in saturation extract ($mmol\,L^{-1}$)								
HCO_3^-	2.24	1.23	4.70	3.48	0.73	0.10	32.47	1.38
Cl^-	47.15	5.28	93.60	88.32	24.40	3.52	51.74	0.14
NO_3^-	nd	nd	nd	nd	–	–	–	–
SO_4^{2-}	261.55	99.55	473.30	373.75	89.68	12.94	34.29	0.52
Cations in saturation extract ($mmol\,L^{-1}$)								
Na^+	260.61	68.72	498.01	429.30	98.06	14.15	37.63	0.32
K^+	1.52	0.50	3.08	2.57	0.61	0.09	40.03	0.36
Ca^{2+}	24.43	20.48	29.38	8.89	2.06	0.30	8.43	0.33
Mg^{2+}	21.95	9.78	55.11	45.33	9.70	1.40	44.17	1.00
Exchangeable cations (mmol/kg)								
Na^+	11.68	1.99	31.15	29.16	5.32	0.77	45.55	1.04
K^+	0.37	0.08	1.29	1.22	0.22	0.03	58.51	2.09
Ca^{2+}	85.69	32.50	160.94	128.45	32.61	4.71	38.06	0.40
Mg^{2+}	4.84	2.38	7.99	5.61	1.54	0.22	31.79	0.46

$N = 48$, nd: all samples below detection limits. Detection limit for NO_3 was $0.04\,mmol\,L^{-1}$.
[a] $N = 40$.

southwest corner. Ground-truth chemical analysis data confirm that the profile ratio from the non-invasive EM EC_a measurements is a reliable means of characterizing the general shape of the EC_a profile.

Tables 1–4 are compilations by depth (0–0.3, 0.3–0.6, 0.6–0.9, and 0.9–1.2 m, respectively) of the basic statistical data characterizing significant physico-chemical properties of soil quality for an arid-zone soil. The mean, minimum, and maximum values indicate that the soil in the study area is severely saline and sodic with heavy texture at the surface (0–0.3 m), low to very high levels of B, and moderate to high levels of Mo. Typically, water content increases with depth (Tables 1–4). Bulk density is the lowest in the top depth increment (0–0.3 m) with an average value of $1.29\,Mg\,m^{-3}$ and is stable at $1.51\,Mg\,m^{-3}$ for the remaining depths. pH_e typically averages around 7.9 for all depths and usually falls within the range of 7.5–8.5. Saturation percentage ranges from 41 to 123% with the greatest range

Table 4
Mean and range statistics for 0.9–1.2 m sample depth

Soil property	Mean	Minimum	Maximum	Range	S.D.	S.E.	CV	Skewness
θ_v (m^3/m^3)	0.29	0.20	0.51	0.31	0.06	0.01	20.84	1.51
ρ_b ($Mg\,m^{-3}$)	1.51	1.14	1.75	0.61	0.16	0.03	10.70	−0.85
Clay (%)	23.3	11.1	36.9	25.8	6.3	1.1	26.9	0.08
EC_e ($dS\,m^{-1}$)	24.30	7.84	45.30	37.46	8.14	1.18	33.51	0.26
pH_e	8.03	7.20	8.36	1.16	0.22	0.03	2.69	−1.47
SP (%)	61.29	41.12	122.95	81.83	15.28	2.20	24.93	1.91
SAR	57.46	16.51	103.12	86.61	17.96	2.59	31.25	−0.03
ESP (%)	86.20	20.59	163.21	142.62	30.14	4.35	34.97	0.54
B ($mg\,L^{-1}$)	21.71	7.89	39.01	31.12	6.59	0.95	30.36	0.48
Mo ($\mu g\,L^{-1}$)	720.67	240.00	2991.00	2751.00	451.50	65.17	62.65	3.11
CEC (mmol/kg)	14.89	4.89	28.40	23.51	5.76	0.83	38.69	0.74
$CaCO_3$ (g/kg)[a]	1.43	0.02	5.03	5.01	1.24	0.19	86.67	1.27
Gypsum (g/kg)	8.46	0.88	26.95	26.07	5.79	0.84	68.49	1.46
Total C (g/kg)	0.39	0.14	0.87	0.73	0.17	0.02	44.34	0.93
Total N (g/kg)	0.03	0.02	0.08	0.06	0.01	0.00	37.37	2.26
Anions in saturation extract ($mmol\,L^{-1}$)								
HCO_3^-	2.30	1.32	3.65	2.32	0.58	0.08	25.24	0.53
Cl^-	55.55	5.50	108.52	103.03	27.14	3.92	48.86	−0.17
NO_3^-	nd	nd	nd	nd	–	–	–	–
SO_4^{2-}	280.42	96.04	606.10	510.06	106.73	15.41	38.06	0.89
Cations in saturation extract ($mmol\,L^{-1}$)								
Na^+	286.02	68.57	622.16	553.59	116.93	16.88	40.88	0.61
K^+	1.55	0.38	3.41	3.03	0.70	0.10	45.59	0.78
Ca^{2+}	24.98	19.88	29.89	10.01	2.41	0.35	9.64	0.29
Mg^{2+}	22.59	7.84	50.96	43.12	9.81	1.42	43.43	0.92
Exchangeable cations (mmol/kg)								
Na^+	12.05	3.07	21.78	18.71	4.20	0.61	34.81	-0.07
K^+	0.29	0.06	0.79	0.73	0.16	0.02	55.59	0.89
Ca^{2+}	88.03	26.14	158.60	132.47	37.02	5.34	42.05	0.05
Mg^{2+}	4.81	2.35	9.38	7.03	1.80	0.26	37.52	0.98

$N = 48$, nd: all samples below detection limits. Detection limit for NO_3 was 0.04 $mmol\,L^{-1}$.
[a] $N = 43$.

occurring at the bottom depth (0.9–1.2 m). The levels of Se and As are very low at all depth increments.

The general spatial patterns of Cl^- (Fig. 4b) and SAR (Fig. 5a) tend to be associated with EC_e (Fig. 4a) and like EC_e, tend to increase with depth (see Tables 1–4). The association between salinity (EC_e) and the soil chemical properties of Cl^- and SAR is reflected by correlation coefficients determined for EC_e and Cl^- ($r = 0.84$), and for EC_e and SAR ($r = 0.97$) using values for composite soil cores over the depth of 0–1.2 m.

Fig. 5b shows that in general the clay content tends to decrease with depth. The average % clay for the 0–0.3 m depth increment is 35.9% and gradually decreases to 23.3% at the 0.9–1.2 m depth increment (see Tables 1–4). The higher clay content at the surface will enhance the formation of surface cracks, which will likely serve as conduits for water flow before the clay swells and closes the cracks. The averages of % sand, % silt, and % clay for

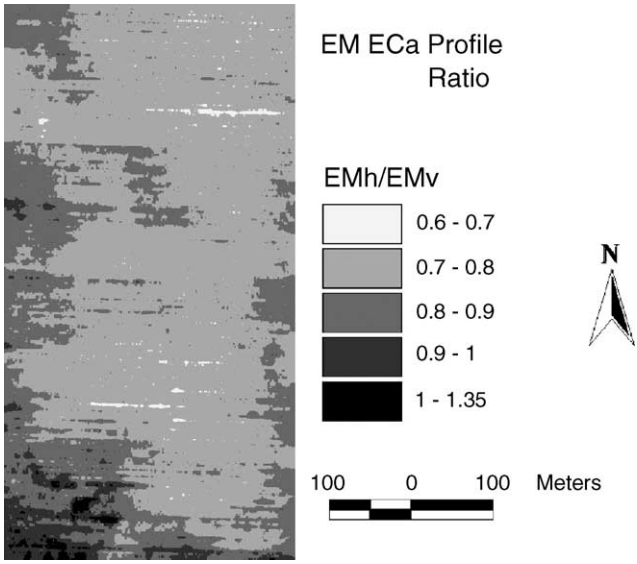

Fig. 3. IDW interpolated map of the EM EC_a profile ratio (i.e., EM_h/EM_v) for all 22,177 EM measurement sites.

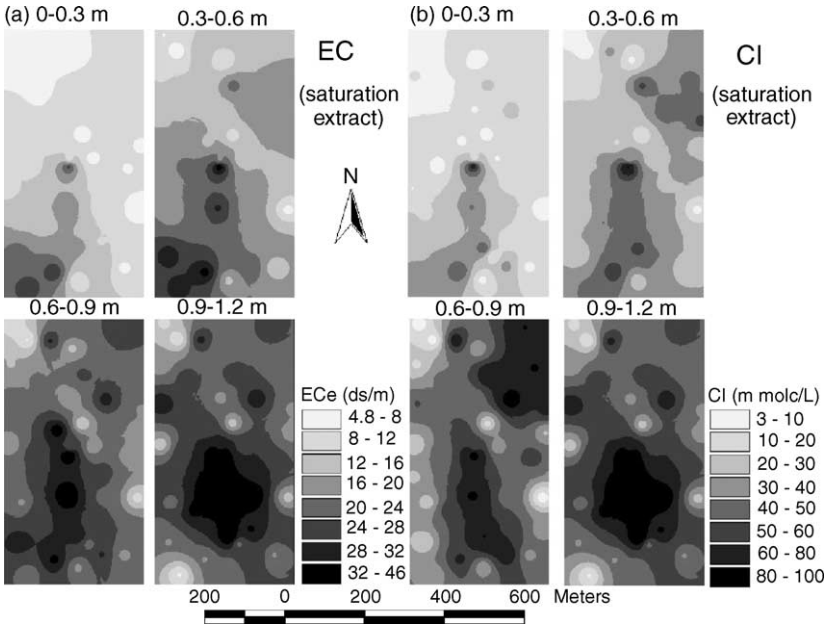

Fig. 4. IDW interpolated maps of (a) EC_e (dS m^{-1}) and (b) Cl^- (mmol L^{-1}) taken at 40 sites for the depths of 0–0.3, 0.3–0.6, 0.6–0.9, and 0.9–1.2 m.

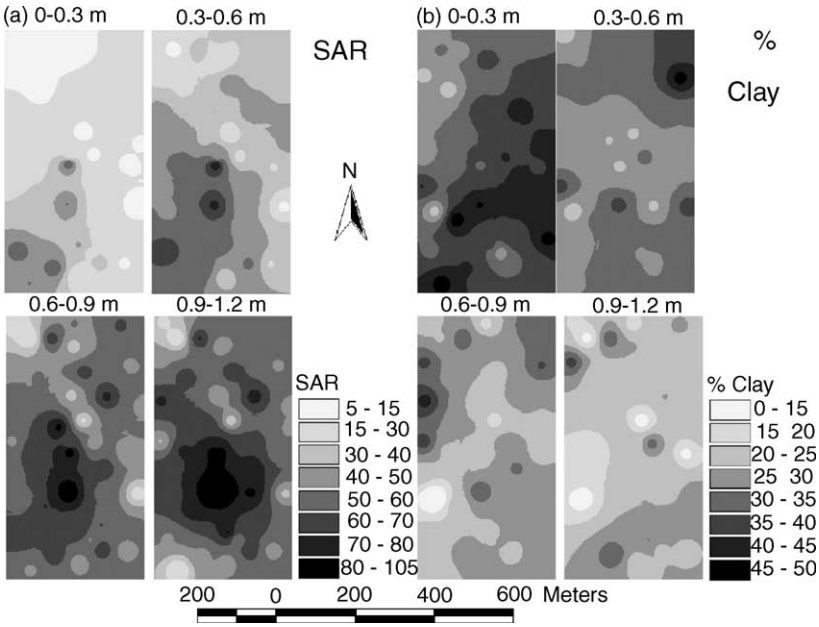

Fig. 5. IDW interpolated maps of (a) SAR and (b) % clay taken at 40 sites for the depths of 0–0.3, 0.3–0.6, 0.6–0.9, and 0.9–1.2 m.

the top 0–1.2 m are 38.6, 32.4, and 29.0%, respectively, classifying the soil as a clay loam. The silt content tends to remain fairly constant through the root zone with values of 32.8, 31.1, 31.3, and 34.5% for the respective depths of 0–0.3, 0.3–0.6, 0.6–0.9, and 0.9–1.2 m. However, sand content tends to increase with depth with values of 31.3, 38.5, 42.5, and 42.2% for the respective depths of 0–0.3, 0.3–0.6, 0.6–0.9, and 0.9–1.2 m. The increase in the sand fraction with depth should be conducive to drainage.

The general spatial patterns of B and Mo (Fig. 6a and b, respectively) tend to coincide in the top two depths (0–0.3 and 0.3–0.6 m). The correlation coefficient between B and Mo using values for composite soil cores over the depth of 0–1.2 m is $r = 0.61$ ($p < 0.0001$). The high levels of B in the shallow depths (0–0.3 and 0.3–0.6 m) of the southwest corner of the field (Fig. 6a) pose a potential threat to continued forage growth at the site. High levels of Mo in the southwest corner at all depths (Fig. 6b) define areas where Mo uptake by the forage crop can pose a threat to ruminant animals. Except for a high mean concentration at 0–0.3 m, Mo tends to increase with depth similar to EC_e (see Tables 1–4). The high levels of B and Mo, particularly near the soil surface (i.e., 0–0.3 m) in the southwest corner, are areas of concern. In irrigated agriculture, it has been recommended that concentrations of Mo not exceed 0.01 mg L^{-1} for continuous application on all soils, or 0.05 mg L^{-1} for short-term use on soils that react with Mo (National Academy of Sciences, 1973). More recently, Albasel and Pratt (1989) recommended a guideline of 0.05 mg L^{-1} maximum Mo concentration for saline SO_4^{2-} dominated waters used on alkaline soils of the WSJV for the protection of bovine animals.

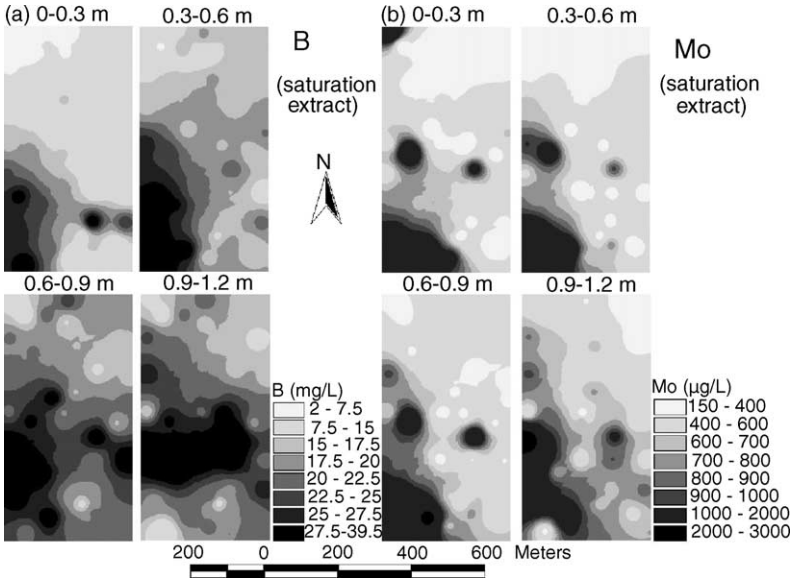

Fig. 6. IDW interpolated maps of (a) B (mg L^{-1}) and (b) Mo (µg L^{-1}) taken at 40 sites for the depths of 0–0.3, 0.3–0.6, 0.6–0.9, and 0.9–1.2 m.

The spatial patterns of K^+, Mg^{2+}, Na^+, and SO_4^{2-} concentrations in the saturation extract tend to follow one another (see Figs. 7 and 8) and follow those of EC_e and Cl^- (see Fig. 4). The concentrations of K^+, Mg^{2+}, Na^+, and SO_4^{2-} expectantly correlate with EC_e and have correlation coefficients of 0.90, 0.74, 0.99, and 0.98, respectively. At shallow depths (i.e., 0–0.3 and 0.3–0.6 m) concentrations of K^+, Mg^{2+}, Na^+, and SO_4^{2-} generally tend to decrease from southwest to northeast, while the deepest depth sampled (i.e., 0.9–1.2 m) shows a pocket of the field's highest concentrations occurring near the middle of the southern half of the field. Concentrations of K^+, Mg^{2+}, Na^+, and SO_4^{2-} tend to increase with depth (see Tables 1–4).

The soil chemistry, particularly in the southern half of the field, is dominated by Na_2SO_4, which results in a high SAR (i.e., SAR: 50–105). The high SAR causes the soil to be dispersed, which has a significant influence on the ability of water to move through the soil. Caution must be taken when irrigating. To enhance the movement of irrigation water through this soil, irrigation water with an EC >3–4 dS m^{-1} is needed.

Compared to other locations in the WSJV (Deverel et al., 1984; Deverel and Fujii, 1988; Deverel and Millard, 1988; Fujii and Deverel, 1989; Fujii and Swain, 1995), sample B and Mo levels are representative, while salinity (EC_e) and SAR levels are high. However, there are specific sample locations within the study site with large amounts of B and Mo. From a global perspective (U.S. Salinity Laboratory Staff, 1954; Lindsay, 1979; Kabata-Pendias and Pendias, 1992), the salinity, SAR, B, and Mo tend to be above average to high.

Total C and total N are very low (Tables 1–4), which is typical of WSJV soils. Soil organic matter tends to rapidly decompose due to the high year-round temperatures. In general, NO_3^- levels in the saturation extract tend to be extremely low with the

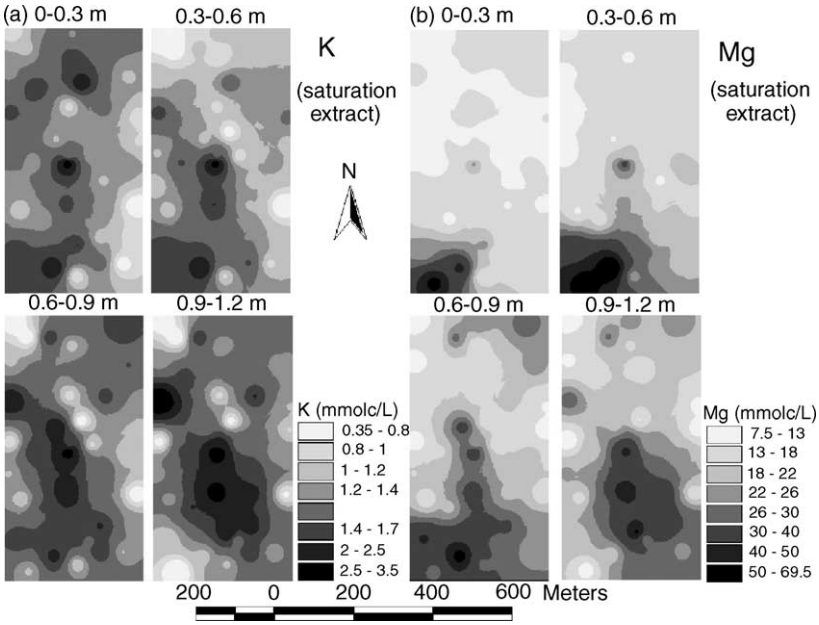

Fig. 7. IDW interpolated maps of (a) K^+ (mmol L^{-1}) and (b) Mg^{2+} (mmol L^{-1}) taken at 40 sites for the depths of 0–0.3, 0.3–0.6, 0.6–0.9, and 0.9–1.2 m.

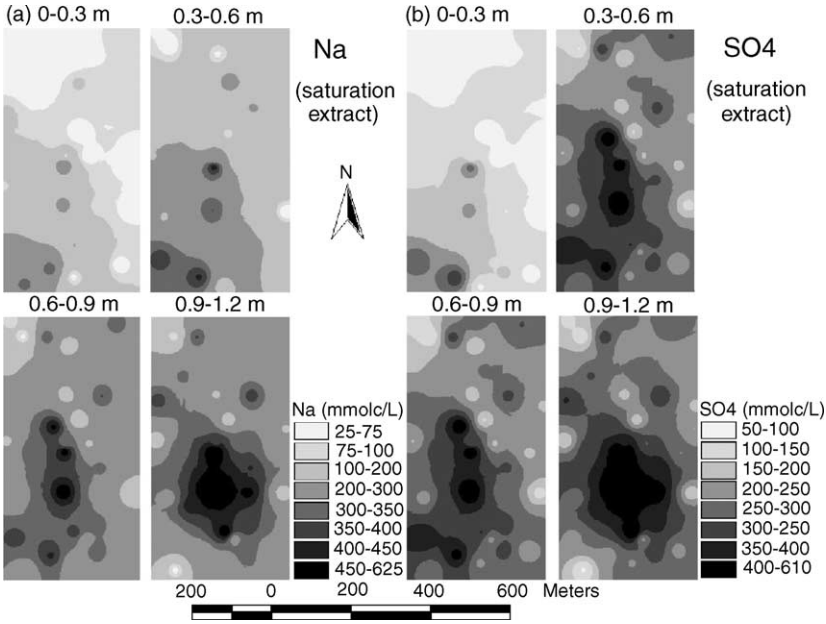

Fig. 8. IDW interpolated maps of (a) Na^+ (mmol L^{-1}) and (b) SO_4^{2-} (mmol L^{-1}) taken at 40 sites for the depths of 0–0.3, 0.3–0.6, 0.6–0.9, and 0.9–1.2 m.

Table 5
Percent local-scale variation of soil properties by depth

Soil property	Soil depth increment (m)			
	0–0.3	0.3–0.6	0.6–0.9	0.9–1.2
θ_v (m^3/m^3)	5.3	5.9	3.9	2.1
ρ_b ($Mg\,m^{-3}$)	1.5	1.7	2.7	2.4
Clay (%)	13.8	20.4	13.6	8.6
EC_e ($dS\,m^{-1}$)	0.8	1.6	5.5	2.8
pH_e	7.1	2.2	14.4	9.1
SP (%)	2.1	2.8	5.8	0.9
SAR	1.0	1.3	3.7	2.1
ESP (%)	5.0	36.8	10.9	15.8
B ($mg\,L^{-1}$)	9.8	2.6	3.3	2.8
Mo ($\mu g\,L^{-1}$)	10.3	0.7	5.1	3.1
CEC (mmol/kg)	10.8	25.1	9.9	2.0
$CaCO_3$ (g/kg)	6.5	14.1	0.5	6.4
Gypsum (g/kg)	10.9	4.7	11.5	5.8
Total C (g/kg)	4.6	5.7	2.8	6.6
Total N (g/kg)	4.8	5.6	8.2	1.2
Anions in saturation extract ($mmol\,L^{-1}$)				
HCO_3^-	9.3	3.7	5.9	5.0
Cl^-	1.6	3.0	5.2	3.4
NO_3^-	–	–	–	–
SO_4^{2-}	0.9	1.1	4.5	2.3
Cations in saturation extract ($mmol\,L^{-1}$)				
Na^+	0.9	1.4	4.9	2.5
K^+	3.5	1.5	5.1	1.9
Ca^{2+}	15.1	2.2	5.7	3.7
Mg^{2+}	1.1	2.3	7.8	3.9
Exchangeable cations (mmol/kg)				
Na^+	2.7	4.0	4.8	4.0
K^+	6.8	5.6	2.8	2.4
Ca^{2+}	2.2	0.9	7.7	3.5
Mg^{2+}	3.8	1.4	4.5	0.5

NO_3^- concentration for the top 0–1.2 m of soil below detection limits for 44 out of 48 samples.

A comparison of the coefficients of variation (CV) for various sample chemical and physical properties at each of the four depth increments shows a range of spatial variability with some general qualitative trends (see Tables 1–4). The properties of % $CaCO_3$ and Mo consistently have the highest sample CVs. Anions and cations in the saturation extract, except Ca^{2+}, exchangeable cations, SAR, ESP, EC_e, B, CEC, and total C have moderate sample CVs (i.e., CVs ranging from about 30–60). Clay percentage, ρ_b, θ_v, SP, and total N have low sample CVs (i.e., CVs < 30) with pH_e, and Ca^{2+} in the saturation extract consistently having the lowest sample CVs (CVs < 10).

The partitioning of the local- and global-scale variability using one-way ANOVA on duplicate composite (0–1.2 m) soil samples indicates that the highest local-scale variability

Table 6
Correlation coefficients between EM EC_a (both EM_h and EM_v) and soil properties measured over 0–1.2 m and $N = 40$

Soil property	EM_h EC_a	95% LCL	95% UCL	EM_v EC_a	95% LCL	95% UCL
θ_v (m^3/m^3)	0.09	−0.23	0.40	0.13	−0.20	0.43
ρ_b ($Mg\,m^{-3}$)	−0.34	−0.59	−0.03	−0.30	−0.56	0.02
Clay (%)	0.33	0.01	0.59	0.28	−0.04	0.55
EC_e ($dS\,m^{-1}$)	0.89**	0.80	0.94	0.84**	0.71	0.91
pH_e	0.40**	0.09	0.64	0.43**	0.13	0.66
SP (%)	0.22	−0.10	0.50	0.30	−0.02	0.56
SAR	0.84**	0.71	0.91	0.82**	0.68	0.90
ESP (%)	0.28	−0.04	0.55	0.30	−0.02	0.56
B ($mg\,L^{-1}$)	0.43**	0.13	0.66	0.40**	0.09	0.64
Mo ($\mu g\,L^{-1}$)	0.25	−0.07	0.53	0.10	−0.22	0.40
CEC (mmol/kg)	0.37*	0.06	0.62	0.33*	0.01	0.59
$CaCO_3$ (g/kg)	−0.28	−0.55	0.04	−0.28	−0.55	0.04
Gypsum (g/kg)	0.13	−0.20	0.43	0.10	−0.22	0.40
Total C (g/kg)	−0.40**	−0.64	−0.09	−0.29	−0.56	0.03
Total N (g/kg)	−0.21	−0.49	0.12	−0.08	−0.39	0.24
Anions in saturation extract ($mmol\,L^{-1}$)						
HCO_3^-	0.56**	0.30	0.75	0.59**	0.34	0.76
Cl^-	0.77**	0.60	0.87	0.81**	0.66	0.90
NO_3^-	–	–	–	–	–	–
SO_4^{2-}	0.87**	0.76	0.93	0.79**	0.63	0.89
Cations in saturation extract ($mmol\,L^{-1}$)						
Na^+	0.88**	0.78	0.94	0.83**	0.70	0.91
K^+	0.74**	0.55	0.86	0.71**	0.51	0.84
Ca^{2+}	0.07	−0.25	0.38	0.13	−0.20	0.43
Mg^{2+}	0.74**	0.55	0.86	0.61**	0.36	0.78
Exchangeable cations (mmol/kg)						
Na^+	0.68**	0.46	0.82	0.68**	0.46	0.82
K^+	−0.13	−0.43	0.20	−0.01	−0.33	0.31
Ca^{2+}	0.12	−0.21	0.42	0.15	−0.18	0.45
Mg^{2+}	0.14	−0.19	0.44	0.12	−0.21	0.42

LCL, lower confidence limit; UCL, upper confidence limit.
* Significant at $P \leq 0.05$ level.
** Significant at $P \leq 0.01$ level.

is for the properties of ESP, % clay, and CEC, while the lowest is for SAR, and Na^+ and SO_4^{2-} in the saturation extract (Table 5). The local-scale variability of ESP is the highest at 17.1%, which indicates that 17.1% of the variability of the entire 32.4-ha field can be found within 1 m. At the other extreme, the local-scale variability of SAR is only 2%. It should be noted that the local-scale variability includes variation in reproducibility in methodology.

Correlations between EM EC_a measurements (both EM_h and EM_v EC_a) and various soil sample properties show that EC_e; Cl^-, SO_4^{2-}, Na^+, K^+, and Mg^{2+} in the saturation extract; and SAR are highly correlated ($r > 0.7$), while pH_e, B, and CEC are less positively correlated, but still significant at the $P \leq 0.05$ level (Table 6). A modest positive correlation exists between EM EC_a and exchangeable Na^+. These correlations suggest that the

EC_a-based sample design utilized in this study will provide the best spatial representation for these sample properties, whereas a grid, random, or stratified random sample design probably would have been better for the remaining properties. Because many of the properties correlated to EC_a are also those of greatest significance for arid zone soil quality, the sample design is not compromised, but sample design modifications would likely improve the spatial characterization of the poorly correlated properties (i.e., θ_v; ρ_b; % clay; SP; ESP; Mo; $CaCO_3$; gypsum; total N; Ca^{2+} in the saturation extract; and exchangeable K^+, Ca^{2+}, and Mg^{2+}).

Extremely low K_s values are typical of soils in the WSJV and are a primary soil quality factor for evaluation. Saturated hydraulic conductivity had been measured at the study site in a soil property assessment conducted in 1999 (Corwin et al., 2003). Both field and laboratory measurements of K_s were made. Field measurements ranged from 0.49 to 1.79 cm h^{-1}, while laboratory K_s ranged from 0.003 to 0.05 cm h^{-1}. The discrepancy was attributed to the difference in the soil volume measured, which introduced anisotropic effects, and to the difference in the vertical location of the soil being measured. Nevertheless, K_s is low and considered an important factor to the soil's management (Corwin et al., 2003).

4. Summary and conclusions

The protocols outlined in part I provide detailed steps for conducting an EC_a survey that provides a priori spatial information about soil physico-chemical properties crucial to soil quality, particularly of arid zone soils. From this spatial information, a soil sample design is developed that reflects the spatial patterns, but minimizes clustering of samples. The methodology lends itself to assessing spatio-temporal change in soil quality since the rapid, reliable measurement of EC_a provides an intensive spatial database for comparative analysis.

To demonstrate the protocols, a case study (part II) was presented of a soil quality assessment. The soil quality assessment was conducted on a research site located in the WSJV, which is representative of land in the vicinity that has been taken out of agricultural productivity because profitable crop yields were unobtainable due to poor soil quality. To conduct the soil quality assessment, outlined protocols for conducting a field-scale EC_a survey were used with a response-surface sampling design strategy adapted from Lesch et al. (1995b, 2000).

The site was found to have elevated levels of soil salinity and sodicity, and sporadically high levels of the trace elements B and Mo in the southwest corner. Even though the site has limited agricultural prospects, it is suited for the production of adapted salt-tolerant forage crops, if adequate infiltration and leaching can be maintained, and excessive amounts of trace elements do not accumulate in forages. The soil quality information that was obtained can be used in comparison to other arid locations throughout the world and to direct and evaluate appropriate management to assure sustainability and profitability.

Several factors are important to manage and sustain the agricultural viability of the study site based on the characterized soil variability and quality. Foremost are the restricted water flow and high soil salinity. Water flow is restricted by the low hydraulic conductivity of the predominantly montmorillonitic clay soil and the influence of dispersion on infiltration due

to Na^+ accumulation. High salinity levels limit the site to only the hardiest salt-tolerant crops of which salt-tolerant forages are the most suitable. Due to elevated levels, the management of salinity, SAR, B, and Mo levels are long-term chemical concerns. Sustainability at the site depends on maintaining a leaching fraction that prevents the accumulation of excessive salinity, Na^+, B, and Mo to prevent the occurrence of toxic effects upon forage and grazing livestock, and yet low enough to meet the objectives of minimizing drainage volumes and the dissolution of additional salts and minerals. Particular concern with respect to salinity, infiltration and permeability, and trace elements can be focused on the middle of the southern half of the field where EC_e, Na^+, B, and Mo are at their highest levels.

The response-surface sampling design has strengths and limitations, which became apparent, but the utility of this approach to assess soil quality of an arid zone soil was demonstrated. The response-surface sampling design provides a practical means of assessing arid-zone soil quality at field scale when the soil quality properties are correlated with EC_a. At the Westlake Farm site the correlated properties (i.e., EC_e; Cl^-, $HCO_3{}^-$, $SO_4{}^{2-}$, Na^+, K^+, and Mg^{2+} in the saturation extract; exchangeable Na^+; SAR; pH_e, B, and CEC) include many soil properties associated with soil quality of arid zone soils, particularly in the WSJV. However, a number of soil properties (i.e., θ_v; ρ_b; % clay; SP; ESP; Mo; $CaCO_3$; gypsum; total N; Ca^{2+} in the saturation extract; and exchangeable K^+, Ca^{2+}, and Mg^{2+}) did not correlate well with EC_a measurements. As a result, the spatial distribution of these poorly correlated properties would not be well represented with a response-surface sampling design. This suggests that a combined and random (or stratified random) sampling design using geo-referenced EC_a measurements is necessary for this site.

Acknowledgements

The authors wish to acknowledge the University of California Kearney Foundation of Soil Science for the funds supporting the soil physical and chemical analyses for the case study soil quality assessment and the assistance of Dr. Stephen Kaffka and Dr. James Oster. Ceil Howe, Jr., and Ceil Howe, III provided the site. The authors thank Nahid Vishteh and Harry Forster for their analytical technical support. Finally, the authors acknowledge the conscientious work and diligence of Clay Wilkinson and Derrick Lai, who performed the physical and chemical analyses. The authors also thank the three anonymous reviewers for their constructive comments, which helped to improve the quality of this paper.

References

Albasel, N., Pratt, P.F., 1989. Guidelines for molybdenum in irrigation waters. J. Environ. Qual. 18, 259–264.

Corwin, D.L., Kaffka, S.R., Hopmans, J.W., Mori, Y., Lesch, S.M., Oster, J.D., 2003. Assessment and field-scale mapping of soil quality properties of a saline-sodic soil. Geoderma 114 (34), 231–259.

Corwin, D.L., Lesch, S.M., 2003. Application of soil electrical conductivity to precision agriculture: theory, principles, and guidelines. Agron. J. 95 (3), 455–471.

Corwin, D.L., Lesch, S.M., 2005a. Apparent soil electrical conductivity measurements in agriculture. Comput. Electron. Agri. 46, 11–43.

Corwin, D.L., Lesch, S.M., 2005b. Characterizing soil spatial variability with apparent soil electrical conductivity. Part I: Survey protocols. Comput. Electron. Agri. 46, 103–133.

Deverel, S.J., Fujii, R., 1988. Processes affecting the distribution of selenium in shallow ground water of agricultural areas, western San Joaquin Valley. California Water Resour. Res. 24, 516–524.

Deverel, S.J., Gilliom, R.J., Fujii, R., Izbicki, J.A., Fields, J.C., 1984. Areal distribution of selenium and other inorganic constituents in shallow ground water of the San Luis Drain Service Area, San Joaquin Valley, California: a preliminary study. U.S. Geol. Surv. Water Resour. Invest. Rept., 84–4319.

Deverel, S.J., Millard, S.P., 1988. Distribution and mobility of selenium and other trace elements in shallow ground water of the western San Joaquin Valley, California. Environ. Sci. Technol. 22, 697–702.

ESRI, 2002. ArcView 3.3. ESRI, Redlands, CA.

Fujii, R., Deverel, S.J., 1989. Mobility and distribution of selenium and salinity in groundwater and soil of drained agricultural fields, Western San Joaquin Valley of California. In: Jacobs, L.W. (Ed.), Selenium in Agriculture and the Environment. SSSA Special Publication No. 23. SSSA, Madison, WI, USA, pp. 195–212.

Fujii, R., Swain, W.C., 1995. Areal Distribution of Selected Trace Elements, Salinity, and Major Ions in Shallow Groundwater, Tulare Basin and Southern San Joaquin Valley. USGS Water Resources Investigations Report 95-4048. USGS, Sacramento, CA, USA.

Kabata-Pendias, A., Pendias, H., 1992. Trace Elements in Soils and Plants, second ed. CRC Press, Boca Raton, FL, USA.

Kaffka, S.R., Corwin, D.L., Oster, J.D., Hopmans, J., Mori, Y., van Kessel, C., van Groenigen, J.W., 2002. Using Forages and Livestock to Manage Drainage Water in the San Joaquin Valley: Initial Site Assessment Kearney Foundation Report. University of California, Berkeley, CA, USA, pp. 88–110.

Klute, A. (Ed.), 1986. Methods of Soil Analysis. Part 1: Physical and Mineralogical Methods, second ed. Agronomy Monograph No. 9. ASA-SSSA, Madison, WI, USA.

Lesch, S.M., Rhoades, J.D., Corwin, D.L., 2000. ESAP-95 Version 2.10R: User Manual and Tutorial Guide. Research Report 146. USDA-ARS George E. Brown, Jr. Salinity Laboratory, Riverside, CA, USA.

Lesch, S.M., Strauss, D.J., Rhoades, J.D., 1995a. Spatial prediction of soil salinity using electromagnetic induction techniques: 1. Statistical prediction models: a comparison of multiple linear regression and cokriging. Water Resour. Res. 31, 373–386.

Lesch, S.M., Strauss, D.J., Rhoades, J.D., 1995b. Spatial prediction of soil salinity using electromagnetic induction techniques. Part 2: An efficient spatial sampling algorithm suitable for multiple linear regression model identification and estimation. Water Resour. Res. 31, 387–398.

Lindsay, W.L., 1979. Chemical Equilibria in Soils. Wiley, New York, NY, USA.

National Academy of Sciences, 1973. Water quality criteria 1972. Committee on Water Quality Criteria, EPA R3-73-033 (1973). U.S. Government Printing Office, Washington, DC, USA.

Page, A.L., Miller, R.H., Keeney, D.R. (Eds.), 1982. Methods of Soil Analysis. Part 2: Chemical and Microbiological Properties, second ed. Agronomy Monograph No. 9. ASA-SSSA, Madison, WI, USA.

Soil Survey Staff, 1999. Soil Taxonomy—A Basic System of Soil Classification for Making and Interpreting Soil Surveys, second ed. USDA Natural Resources Conservation Service Agricultural Handbook 436. U.S. Government Printing Office, Washington, DC, USA.

Sudduth, K.A., Drummond, S.T., Kitchen, N.R., 2001. Accuracy issues in electromagnetic induction sensing of soil electrical conductivity for precision agriculture. Comput. Electron. Agri. 31, 239–264.

USDA, 1986. Soil Survey of Kings County, CA. Sheet No. 7, p. 43. USDA, Soil Conservation Service, Washington, DC, USA.

U.S. Salinity Laboratory Staff, 1954. Diagnosis and improvement of saline and alkali soils, USDA Handbook 60. U.S. Government Printing Office, Washington, DC, USA, pp. 1–160.